PHYSICAL REVIEW B **68**, 241401(R) (2003)

Shapes of cagelike metal carbide clusters: First-principles calculations

G. K. Gueorguiev[1] and J. M. Pacheco[2]
[1]*Departamento de Física da Universidade, P-3004-516 Coimbra, Portugal*
[2]*Centro de Física Teórica e Computacional, Departamento de Física da Faculdade de Ciências, Complexo Interdisciplinar da Universidade de Lisboa, Avenida Prof. Gama Pinto 2, P-1649-003 Lisboa Codex, Portugal*

(Received 27 July 2003; revised manuscript received 25 September 2003; published 3 December 2003)

The infrared spectra of the metcars X_8C_{12} with $X=$V, Nb, Zr, in the gas phase, recently determined experimentally using the infrared resonance enhanced multiphoton ionization technique, are computed from first-principles for several of the lowest-energy local minima found for these clusters. By comparing the experimental spectra and the theoretical results, we assign the dominant shape of each cluster species present in the molecular beams. It is found that the most abundant species corresponds to a T_d-like shape which also coincides, in all cases, with the equilibrium structure found via first-principles unconstrained optimization. The occurrence of absorption strength in regions not accountable for theoretically indicates that other structures, associated with low-lying isomers, coexist with the ground-state conformation in the beams.

DOI: 10.1103/PhysRevB.68.241401 PACS number(s): 61.46.+w, 33.20.Ea, 36.40.−c

Gas-phase metal carbide clusters appear in a variety of stoichiometries and with different structures. Yet, until recently mostly indirect evidence on their shapes had been gathered making use of several techniques, namely, the analysis of abundance spectra, photofragmentation,[1,2] photoionization in combination with quantum chemical calculations,[3,4] or gas-phase ion chromatography[5,6] (a notable exception is Ref. 7, in which a direct comparison between calculated and measured vibrational spectra of Nb_3C_2 has been carried out). Also, reactions with chlorine, oxygen, carbon monoxide, and various organic molecules have been used to probe the coordination of the ''surface'' atoms of clusters.[8–10] More recently, application of the infrared resonance enhanced multiphoton ionization (IR-REMPI) technique to determine the IR-vibrational spectra of the titanium metcar Ti_8C_{12} (Ref. 11) as well as of small titanium and vanadium carbide nanocrystals starting with the $X_{14}C_{13}$ stoichiometry[12,13] has been employed with success.

As is well known, the vibrational spectrum of a molecule or cluster is intimately related to its underlying structure. As such one can, in principle, relate the IR spectra with a well-defined shape. This has been worked out in Ref. 14 for Ti_8C_{12}, in which a direct comparison between the IR experimental data on gas phase Ti_8C_{12} and the IR spectra obtained from first-principles computer simulations has been carried out, providing an efficient way of assigning a specific structure to a given IR spectrum. In carrying out this comparison, however, one must not overlook the fact that the clusters present in the molecular beam have a sizeable vibrational temperature. Furthermore, it is well known that the potential-energy surface (PES) of a cluster is a highly nonlinear function of the atomic coordinates, in which the lowest-energy state typically lies within a plethora of local minima. As a result, the high vibrational temperature of the clusters (after IR laser excitation) may allow the coexistence of more than one structure in the beam besides the ground-state conformation, associated with low-energy isomers. This is what happens with Ti_8C_{12},[14] for which the best fit to the experimental data was obtained with a D_{2d}-like structure which does not coincide with the equilibrium structure obtained at $T=0$, with a T_d-like shape.

Recently, the IR spectra of other transition-metal carbide clusters with stoichiometry X_8C_{12}, for $X=$V, Nb, Zr, have been determined experimentally[15] making use of the same IR-REMPI technique which was used with success to determine the IR spectrum of Ti_8C_{12} in the gas phase. All clusters were probed for a frequency window ranging from 1000 to 1600 cm^{-1}, the resulting overall spectral shapes displaying sizeable differences as one changes transition-metal element.

Similar to the case of Ti_8C_{12}, experiment alone is not able to identify the shape of the carbide clusters flying in the molecular beams. Moreover, the high vibrational temperature of the clusters may enable the coexistence of more than one isomer in the beam.

In keeping with these considerations we compute, from first principles, the most likely candidate shapes for each cluster species, and for each of these shapes, we calculate the associated IR spectrum. By carrying out a direct comparison between theory and experiment, we identify the dominant shape of the clusters present in the molecular beams. An essential feature of this procedure relies on the sensitivity of the IR spectra to the cluster shape, as well as on the symmetry differences associated with competing shapes, in spite of their similarity in what concerns energy stability.

The theoretical spectra have been computed using the ADF program package,[16] in which the properties useful to this work were calculated within the generalized gradient approximation to density-functional theory.[14] In practice, one solves the Kohn-Sham equations by projecting them in a finite, localized basis set of Slater-type orbitals. For carbon we used a frozen-core triple ζ basis augmented with two polarization functions to describe the standard four active valence electrons. This choice has proven successful in describing both structural and electronic properties of Ti_8C_{12} (Ref. 14) and fullerenes.[17] For the transition metals we used, in all cases, the best basis set available in ADF. This corresponds to including as active electrons not only the standard valence shell but also the semicore shell right below. The basis set is furthermore augmented with extra diffuse functions. These features are known to be crucial[14,18,19] in ensuring a proper description of the chemical bond for these atoms.

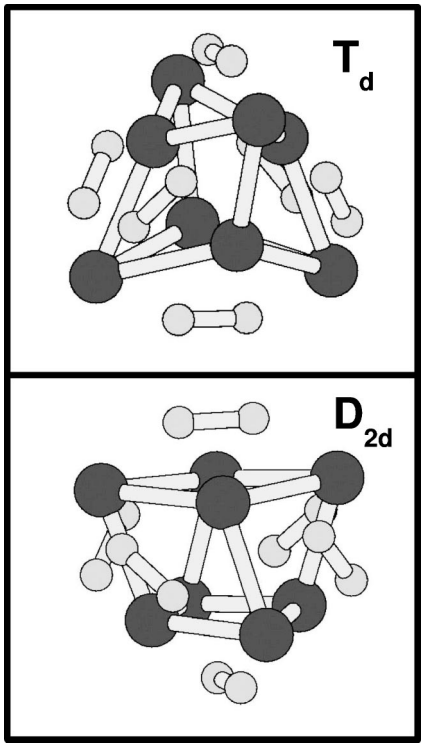

FIG. 1. The two basic, optimized, symmetric seed structures of the metcars studied in this work are depicted, exhibiting T_d (top panel) and D_{2d} (lower panel) symmetries. These structures were used as a starting point for symmetry unconstrained structural optimizations (see main text for details).

For all types of metcars studied here, the geometry optimizations were carried out using both conjugate-gradient and quasi-Newton algorithms (in the latter case with a Broyden-Fletcher-Goldfarb-Shanno Hessian update strategy). Both algorithms provide efficient local optimization strategies, the latter being the default option in ADF.

Within the *ab initio* framework described the vibrational spectrum of a cluster can be determined by diagonalizing the Cartesian displacement matrix explicitly constructed in ADF.

An average of 12 runs (per metcar species) starting from random geometries as well as from educated guesses based on different minima obtained in Ref. 14 has been carried out, in order to avoid trapping in local minima. The runs led to two basic geometries which show up as local minima of the PES, exhibiting a T_d and a D_{2d} symmetry, displayed in Fig. 1. Other local minima were found, namely, associated with the initially proposed[20] T_h symmetry, but these minima had an associated cohesive energy much smaller (between 13 and 15 eV, depending on the transition metal involved) than that of the other two minima depicted in Fig. 1.

Starting from these highly symmetric structures, we tried further reoptimizations—at least 15 runs per symmetric configuration for each metcar species—by inducing random displacements of one or more atoms of the cluster with respect to their equilibrium positions, in this way breaking the intrinsic symmetry associated with the equilibrium shape. After each random perturbation, we performed a geometry optimization of the structures without imposing any symmetry constraints. As a result we obtained several asymmetric local minima of which, for each metcar, we selected the two most stable. These shapes resemble very much, in all cases, the ''seed'' structure used as a reference for perturbation. In contrast with their symmetric seeds, these new minima exhibit no special symmetry, and therefore we label them with reference to the high-symmetry structure that we used as a seed for perturbation, appending a star to distinguish these from the seed structures. Indeed, these new structures amount to small distortions with respect to the symmetric seeds, and as such are difficult to distinguish by eye from the latter. More elucidating information is gathered in Table I. For each metcar, and for each structure, several electronic properties are presented, which reveal in more detail the subtle differences which are induced by the structural rearrangements involved in going from the main shapes of Fig. 1 to the asymmetric local minima. For the T_d-based geometries, the fact that via a Jahn-Teller distortion the system opens up a finite (HOMO, highest occupied molecular orbital; LUMO, lowest unoccupied molecular orbital) HOMO-LUMO gap is rewarded by a corresponding gain in cohesive energy in going from the symmetric T_d shape to the asymmetric T_d^* partner. On the other hand, for the D_{2d}-based minima, which exhibit well-developed HOMO-LUMO (HL) gaps in the symmetric conformation, only for the vanadium (8,12) metcar, one actually obtained an increase of the cohesive energy by distorting the original D_{2d} cage. Overall, the spectra associated with the D_{2d}-based minima were easier to obtain—in other words, convergence took place in fewer iterations—than those associated with the T_d-based minima, a feature which may be related to the smaller HL gaps exhibited by the latter group of shapes. Indeed, large HL gaps are typically associated with local structural stability. In keeping with this discussion, we would like to point out that it is well known that local-density approximation or generalized gradient approximation (GGA) is usually unable to provide reliable estimates for the HL gaps, with absolute errors which can amount to factors of 2 in some semiconducting materials. However, linear-response calculations in both metal and semiconductor clusters, which rely on the detailed energies and relative ordering

TABLE I. Results for the various quantities computed for the four structures of each of the metcars Zr_8C_{12}, V_8C_{12}, and Nb_8C_{12} considered in this work. Besides the HOMO-LUMO gaps, we also tabulate the quantity Δ, which represents the difference in cohesive energy between the most stable structure—in all cases, the T_d^* shape—and the actual structure for each transition metal (see main text for details).

V geometry	D_{2d}	T_d	D_{2d}^*	T_d^*
HOMO-LUMO gap (eV)	0.704	0.000	0.533	0.237
Δ (eV)	1.746	0.332	1.721	0.000
Zr geometry	D_{2d}	T_d	D_{2d}^*	T_d^*
HOMO-LUMO gap (eV)	0.291	0.000	0.331	0.051
Δ (eV)	2.382	0.036	2.389	0.000
Nb geometry	D_{2d}	T_d	D_{2d}^*	T_d^*
HOMO-LUMO gap (eV)	0.529	0.000	0.520	0.428
Δ (eV)	2.445	0.946	2.463	0.000

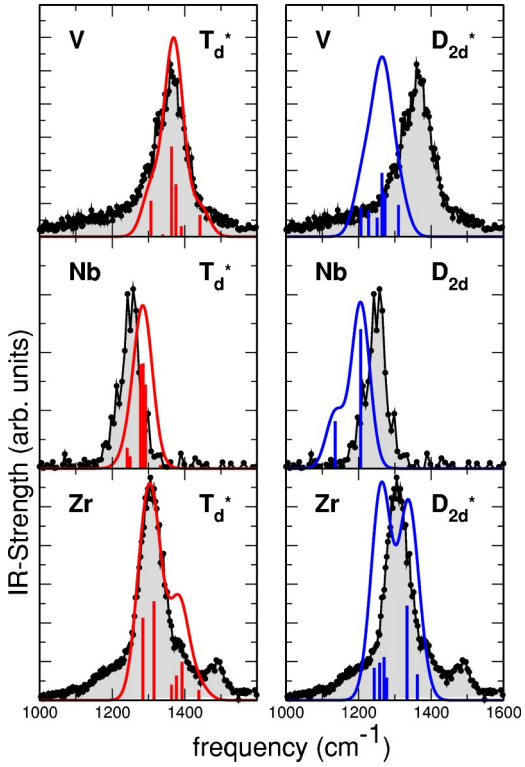

FIG. 2. (Color online) Comparison between the experimental spectra measured with IR REMPI for V_8C_{12} (upper panel), Nb_8C_{12} (middle panel), and Zr_8C_{12} (lower panel), and the IR spectra computed within DFT for the two most stable minima of each class of structures: T_d like (left column) and D_{2d} like (right column). In all panels the experimental data are drawn with solid circles connected by straight solid lines. In order to distinguish better the theoretical and the experimental curves, the area underneath the experimental data has been shaded. As a result of the theoretical calculations, one obtains the sharp spikes shown (scaled so as to make them visible in this arbitrary scale). By folding these sharp spikes (see main text for details) one obtains the solid lines. In all cases, and for all transition metals, the best fit to the experimental spectra was obtained with the theoretical curve associated with the T_d^* structures.

of the electronic energy levels produced by GGA calculations, have shown that one-electron transitions are well accounted for at this level of approximation to density-functional theory (DFT), in spite of the (sometimes) gross errors associated with the HL gaps. Furthermore, the HL gap errors introduced by GGA tend to be systematic, which makes it a feasible tool to predict qualitative trends, as discussed here, in spite of the fact that the absolute values of the HL gaps may not be trustworthy.

In Fig. 2 we compiled the main results of this work. The experimental spectra obtained for the different metcars are depicted with solid circles connected with straight lines. In order to better identify the data, the area underlying the experimental data has been shaded. Each metcar species occupies one row in Fig. 2, and the experimental data are plotted twice along each row to allow for a direct comparison with the theoretical results, displayed with a thick solid line. This line is the result of the computation of the IR spectrum, for each cluster, at the local-minimum shape of the T_d or D_{2d} types which, for a given cluster, best fits the experimental data. Indeed, in the left panels we concentrate on the T_d-like shapes whereas in the right panels we plot the data associated with the D_{2d}-like shapes. The theoretical curves were obtained by replacing the sharp absorption peaks—also plotted in Fig. 2—with normalized Gaussian functions with an intrinsic width of 50 cm^{-1}. To be noted that the vertical scales in Fig. 2 are arbitrary, in the sense that different scaling factors were used for each set of theoretical results shown, in order to (i) make the sharp spikes visible in each panel and (ii) best fit the experimental spectra with the theoretical curves (solid lines). The same fitting criteria determined the value adopted for the intrinsic width of the folding Gaussians. For all metcars studied here, the structure which best describes the experimental data corresponds to the T_d^* structure. However, detailed comparison between the theoretical and experimental profiles indicates clearly the possibility that more than one isomer of the same metcar may be present in the molecular beam. Indeed, a few comments are in order: It is well known that the spectral intensity measured experimentally cannot be directly related to the linear IR absorption intensity computed theoretically. As such, the only meaningful comparison reduces to the peak positions. In this respect one cannot, in general, expect the DFT-based calculations to be 100% reliable, that is, one expects the (theoretically blue shifted) peak obtained for Nb_8C_{12} to fall within the shortcomings of the standard approximations to DFT. However, when one concentrates on the spectra for V_8C_{12} and Zr_8C_{12}, the existence of IR strength is clearly visible which cannot be accounted for by the theoretical spectra associated with only one shape (even if shifted). This feature indeed suggests the coexistence of more than one isomer in the molecular beam. This is further suggested by the results for the zirconium metcar, for which the two T_d-like isomers have an energy difference small enough to render the symmetric T_d shape thermally accessible from a reference T_d^* conformation (to the extent the energy barrier is small), with an IR spectrum which is very similar to the one plotted in Fig. 2, yet with a narrower strength distribution.

For all metcars, besides the results shown in Fig. 2, the theoretical IR spectra contain an appreciable amount of strength also at lower frequencies, in the region around ~ 500 cm^{-1}, the characteristic frequencies at which one expects vibrations associated with the metal atoms. However, the present IR REMPI technique is only effective at higher frequencies for these clusters, where one expects to witness the contributions associated mostly with vibrations of the dicarbon bonds as well as the carbon-metal bonds. Indeed, at this level of approximation—GGA to DFT—the vibrational frequency of the carbon dimer occurs at 1670 cm^{-1} for an intercarbon distance of 2.5 bohrs. These results can be directly compared to the distances between carbon dimers in the T_d^* and D_{2d}^* structures—all at ≈ 2.6 bohrs, which point to an appreciable amount of strength at ≈ 1350 cm^{-1}, as obtained. However, the changes within the transition-metal skeletons when one compares the D_{2d}^* and the T_d^* structures,

and the corresponding modifications of the IR spectra, put in evidence the role played by the carbon-metal coupling in the resulting IR spectrum.

The results obtained show a more narrow distribution for the T_d-like structures as compared to the D_{2d}-like structures. This is, in part, due to the larger number of equivalent sites in the T_d-like shapes, with corresponding degeneracies. Nevertheless, by changing the element one can observe that the IR spectra can change substantially, in spite of the fact that the bond lengths for the dicarbon satellites remain essentially unchanged. Furthermore, changing the element also brings about sizeable changes in the HOMO-LUMO gaps (cf. Table I). The fact that the HOMO-LUMO gap for Zr_8C_{12} is much smaller than the other two may be associated with the broadening of the strength distribution, as exhibited in Fig. 2. Indeed, a similar feature has been observed in the IR spectrum of Ti_8C_{12} associated with the T_d^* shape,[14] which also develops a very small HOMO-LUMO gap.

In summary, the direct comparison between the experimental IR spectra of cagelike metcars involving vanadium, niobium, and zirconium in a molecular beam and first-principles computer simulations of the same spectra for the lowest-energy minima of these systems provides crucial information towards the assignment of the dominant shape of the metcar contributing to the experimental data. The shapes assigned coincide with the ones corresponding to the prediction of the computer simulations for the ground-state structures of these metcars. Detailed comparison between the theoretical and experimental profiles associated with hot clusters, as well as the results obtained previously for Ti_8C_{12}, for which the assignment does not correspond to the ground-state prediction, suggests that other isomers coexist with the dominant shape in the molecular beam of the experimental apparatus. Other minima may be entropically accessible via the vibrational temperature. In order to better test this possibility, as well as the quality of the DFT predictions of the IR spectra of clusters, one should be able to measure the spectra for which the relative intensity could be directly related to the spectral IR absorption intensity computed theoretically. To this end, a deeper understanding of the mechanism of thermionic emission process in clusters is mandatory.

Financial support from Ministry of Science and Technology under Contract No. POCTI/FIS/10019/98 and Grant No. PRAXIS XXI/BD/19578/99 (G.K.G.) is gratefully acknowledged. The authors also thank Deniz van Heijnsbergen and Gert von Helden for providing the experimental data reported here.

[1] J.S. Pilgrim, L.R. Brock, and M.A. Duncan, J. Phys. Chem. **99**, 544 (1995).
[2] J. Purnell, S. Wei, and A.W. Castleman, Jr., Chem. Phys. Lett. **229**, 105 (1994).
[3] L.R. Brock and M.A. Duncan, J. Phys. Chem. **100**, 5654 (1996).
[4] M.W. Heaven, G.M. Stewart, M.A. Buntine, and G.F. Metha, J. Phys. Chem. A **104**, 3308 (2000).
[5] G. von Helden, Nigel G. Gotts, Philippe Maitre, and Michael T. Bowers, Chem. Phys. Lett. **227**, 601 (1994).
[6] S. Lee, N.G. Gotts, G. von Helden, and M.T. Bowers, Science **267**, 999 (1995).
[7] D.-S. Yang, M.Z. Zgierski, A. Bérces, P. Hackett, P.-N. Roy, A. Martinez, T. Carrington, Jr., D.R. Salahub, R. Fournier, T. Pang, and C. Chen, J. Chem. Phys. **105**, 10 663 (1996).
[8] C.S. Yeh, Y.G. Byun, S. Afzaal, S.Z. Kan, S. Lee, B.S. Freiser, and P. Jeffrey Hay, J. Am. Chem. Soc. **117**, 4042 (1995); Y.G. Byun, S.Z. Kan, A.A. Lee, Y.H. Kim, M. Miletic, R.E. Bleil, S. Kais, and B.S. Freiser, J. Phys. Chem. **100**, 6336 (1996); Y.G. Byun, S.A. Lee, S.Z. Kan, and B.S. Freiser, *ibid.* **100**, 14 281 (1996).
[9] H.T. Deng, K.P. Kerns, R.C. Bell, and A.W. Castleman, Jr., Int. J. Mass Spectrom. Ion Processes **167/168**, 615 (1997).
[10] H.T. Deng, K.P. Kerns, and A.W. Castleman, Jr., J. Am. Chem. Soc. **118**, 446 (1998).
[11] D. van Heijnsbergen, G. von Helden, M.A. Duncan, A.J.A. van Roij, and Gerard Meijer, Phys. Rev. Lett. **83**, 4983 (1999).
[12] G. von Helden, A.G.G.M. Tielens, D. van Heijnsbergen, M.A. Duncan, S. Hony, L.B.F.M. Waters, and G. Meijer, Science **288**, 313 (2000).
[13] G. von Helden, D. van Heijnsbergen, M.A. Duncan, and Gerard Meijer, Chem. Phys. Lett. **333**, 350 (2001).
[14] G.K. Gueorguiev and J.M. Pacheco, Phys. Rev. Lett. **88**, 115504 (2002).
[15] G. von Helden, D. van Heijnsbergen, and Gerard Meijer, Am. J. Physiol. **107**, 1671 (2003).
[16] G. te Velde and E.J. Baerends, J. Comput. Phys. **99**, 84 (1992).
[17] G.K. Gueorguiev and J.M. Pacheco, J. Chem. Phys. **114**, 6068 (2001).
[18] J.M. Pacheco, G.K. Gueorguiev, and J.L. Martins, Phys. Rev. B **66**, 033401 (2002).
[19] Carlos L. Reis, M. Sc. thesis, University of Porto, 2001 (unpublished).
[20] B.C. Guo, K.P. Kerns, and A.W. Castleman, Jr., Science **255**, 1411 (1992); B.C. Guo, S. Wei, J. Purnell, S. Buzza, and A.W. Castleman, Jr., *ibid.* **256**, 515 (1992).